Journal of
Nanomedicine & Nanotechnology

Lobo et al. J Nanomedic Nanotechnol 2011, 6:2
DOI: 10.4172/2157-7439.1000277

Research Article Open Access

Influence of Temperature and Time For Direct Hydroxyapatite Electrodeposition on Superhydrophilic Vertically Aligned Carbon Nanotube Films

A.O. Lobo[1,2*], F.R.Marciano[1,2], I. Regiani[3], J.T. Matsushima[4], S.C. Ramos[4] and E.J. Corat[3]

[1]*Laboratório de Nanotecnologia Biomédica, Instituto de Pesquisa e Desenvolvimento, Universidade do Vale do Paraiba (UNIVAP), Av. Shishima Hifumi, 2911, 12244-000, Sao Jose dos Campos, SP, Brazil*
[2]*Laboratório de Espectroscopia Vibracional Biomédica, Instituto de Pesquisa e Desenvolvimento, Universidade do Vale do Paraiba (UNIVAP), Av. Shishima Hifumi, 2911, [1]2244-000, Sao Jose dos Campos, SP, Brazil*
[3]*Instituto Tecnologico de Aeronautica (ITA), Praca Marechal Eduardo Gomes 50, São José dos Campos, 12228-900, SP, Brazil*
[4]*Laboratório Associado de Sensores e Materiais, Instituto Nacional de Pesquisas Espaciais, Av. dos Astronautas 1758, Sao Jose dos Campo/SP, Brazil*

Abstract

Superhydrophilic vertically aligned multi-walled carbon nanotubes were used as substrate to direct hydroxyapatite electrodeposition. Conventional Nickel/Titanium alloys were used for comparison. Results show that the bath temperature and the hydrophobicity control affect the hydroxyapatite/carbon nanotube composites obtained by electrodeposition. These results were proved using X-ray diffraction, Energy-dispersive X-ray spectroscopy, field emission gun scanning electron microscopy and Raman spectroscopy.

Keywords: Carbon nanotubes; Vertically aligned; Superhydrophilic; Nanohydroxyapatite; Electrodeposition

Introduction

Vertically-aligned multi-walled carbon nanotubes (VACNTs) are arousing interest from researchers in biomedical area due to their exceptional combination of mechanical properties, chemical properties, and biocompatibility [1]. Hydrophilic surfaces are generally favorable to cell attachment and biomineralization of bone tissues [2]. In order to create novel nanobiomaterials that mimic bone, it is essential to develop strategies for crystallization under physiological, structural, and morphological friendly conditions. Studies on biomineralization mechanisms have aimed to develop a detailed understanding of interfacial interactions associated with biomineralization and template-directed crystallization [3].

Hydroxyapatite (HA) is a form of calcium phosphate that bears close chemical resemblance with the mineral component of bones and teeth [4]. It promotes tissue adhesion and bone growth by spontaneously forming a biologically active bonelike apatite layer over its surface [5]. Thus, HA is classified as one of the best biocompatible and bioactive materials many biological applications such as bone repair scaffolds [6]. However, its poor mechanical properties such as brittleness and low wear resistance have limited the use of bulk HA coating in implant applications [7]. To tackle this problem, HA composites reinforced with polymers have been used [8,9] with the objective of reinforcing phases in order to achieve the desired mechanical properties.

There is a growing interest in controlling HA crystal nucleation, crystallinity, and growth to assemble composite material which is analogous to those produced by nature, involving biomineralization process [10]. Poor crystallinity can directly affect factors governing natural precipitation of apatite formation to promote natural osteointegration [11]. Therefore, the development of crystalline nano-biomaterials is of particular interest in regenerative medicine.

Some investigations have been performed on the synthesis of HA and carbon nanotubes (CNTs) using various methods, such as simulated body fluid (SBF) [12], composite coatings obtained by electrophoresis [13], and more recently, aerosol deposition [14]. Sol-gel methods have been used to obtain CNTs/HA hybrid composites. However, these methods consist in dispersing CNTs in HA solution [15] and a thermal treatment is necessary to obtain crystalline HA. Vertically-aligned CNT (VACNT) film has been used as scaffold to direct HA deposition. Lifang et al. [16] showed that VACNTs were efficient templates to grown HA films using plasma-enhanced chemical vapor deposition and radio-frequency sputtering deposition, however, the authors clearly showed that the Ca- and P-rich layer consists of a carbonate-containing HA with disordered structure and thus poor crystallinity.

For the preparation of HA coatings by electrochemical synthesis, several factors have to be considered, such as substrate morphology, solution composition, P^H, and deposition temperature. These factors directly affect the purity, crystallinity, stoichiometry, morphology, and mechanical strength of the resulting coatings [17,18].

We have recently shown a new method to obtain crystalline HA/VANCT composites using direct electrodeposition process [19]. Hence this study focuses on how electrochemical experimental conditions, wettability of surfaces, and electrodeposition time can affect crystallinity, thickness, particle size, and morphology of HA films on VACNT. Differences in HA crystal growth were evaluated by X-ray diffraction (DRX), Energy-dispersive X-ray spectroscopy (EDX) and field emission gun scanning electron microscopy techniques. Superhydrophilic VACNT films significantly stimulate the nHA crystal formation without any thermal treatment only in bath temperature at 70°C.

***Corresponding author:** A.O. Lobo, Laboratório de Nanotecnologia Biomédica, Instituto de Pesquisa e Desenvolvimento, Universidade do Vale do Paraiba (UNIVAP), Av. Shishima Hifumi, 2911, 12244-000, Sao Jose dos Campos, SP, Brasil. Tel: +55 12 3947 1166; E-mail: loboao@yahoo.com

Received June 20, 2011; **Accepted** July 28, 2011; **Published** August 01, 2011

Citation: Lobo AO, Marciano FR, Regiani I, Matsushima JT, Ramos SC, et al. (2011) Influence of Temperature and Time For Direct Hydroxyapatite Electrodeposition on Superhydrophilic Vertically Aligned Carbon Nanotube Films. J Nanomedic Nanotechnol 6:277. doi:10.4172/2157-7439.1000277

Materials and Methods

Synthesis of vertically aligned multiwalled carbon nanotubes films

The VACNTs were produced as a thin film, using a microwave plasma chamber (2.45 GHz) [20-22]. The substrates were 10 mm titanium squares, covered by a thin nickel layer (10 nm) deposited by an e-beam evaporator. The nickel layer was pre-treated to promote nanocluster formation, which forms the catalyst for VACNT growth. The pre-treatment was carried out for 5 min in plasma of N_2/H_2 (10/90sccm), at a substrate temperature around 760°C. After pre-treatment, CH_4 (14 sccm) was inserted into the chamber at a substrate temperature of 760°C for 2 min. The reactor was kept at a pressure of 30 Torr during the whole process.

VACNT functionalized by polar groups to obtain superhydrophilicity

Functionalization of the VACNT tips by the incorporation of oxygen-containing groups was performed in a pulsed-direct current plasma reactor with an oxygen flow rate of 1 sccm, at a pressure of 85 mTorr, -700 V and with a frequency of 20 kHz [23].

A chemical surface modification was calculated using liquids with different surface tensions and polarities as shown and calculated elsewhere [23].

Hydroxyapatite electrodeposition process on VACNT

The electrodeposition of HA crystals on VACNT films was performed using 0.042 $molL^{-1}$ $Ca(NO_3)_2.4H_2O$ + 0.025 $molL^{-1}$ $(NH_4).2HPO_4$ electrolytes (P^H =4.7). The electrochemical measurements were made using a three-electrode cell coupled to Autolab PGSTAT 302 equipment. Superhydrophilic and as-grown VACNT films were used as working electrode, and the geometric area in contact with electrolytic solution was 0.27cm^2. A platinum coil wire served as auxiliary electrode and Ag/AgCl electrode was used as reference electrode. A cyclic voltammetry study was carried out using the previously described solution in order to determine the parameters for electrodeposition of HA films on superhydrophilic and as-grown VACNT. The cyclic voltammogram was obtained by scanning the potential between 0.5 and -2.5 V at a scan rate of 10 mV s^{-1}. Based on the cyclic voltammetry results, HA films were produced applying a constant potential of -2.0 for different electrodeposition conditions, for periods of 20, 30, and 120 min; and batch temperatures at 23 and 70°C. All these parameters and conditions were used to evaluate the crystal formation and evolution current differences of HA electrodeposition process.

Characterization of functionalized VACNT and HA crystals

SEM (field emission gun, JEOL JSM-6330F) was used to observe the structure of VACNTs and HA crystal morphologies. The elemental composition of the coating was investigated by energy-dispersive x-ray. The structural analysis of HA crystals was performed by DRX diffractometer (X-Pert Philips) with Cu Ka radiation generated at 40 kV and 50 mA. Raman spectroscopy (Renishaw micro-Raman model 2000 with Ar laser, λ = 514.5 nm) measurements were carried out to analyze the chemical composition of HA coatings.

Results and Discussion

The electrochemical deposition temperature (hydrothermal processing) was varied to improve the HA content of the coatings. The transient of cathodic current may be divided in two periods. Initially, a rapid increase of cathodic current due to electric double-layer charging was observed.

Figure 1a and Figure 1b show the difference between evolutions of the current as a function of deposition time of HA on superhydrophilic VACNT films in 23 and 70°C (bath temperature). NiTi alloys were used as control.

A rapid increase of cathodic current due to electric double-layer charging (region 1) was observed (Figure 1a) for all the substrates. However, no cathodic current difference between NiTi and superhydrophilic VACNT was observed when the temperature of the solution was kept in 23°C (approximate value of 0.25 mA). We observed higher current values when the temperature of the solution was kept at 70°C. By comparing superhydrophilic VACNT and NiTi alloys, it was clearly observed a higher current value for superhydrophilic VACNT serving as an electrode (-0.60 mA).

During the second period (region 2), the current value slowly decreased to a limit value, indicating that hydroxyl ion generation process due to the reduction of water and dissolved oxygen on nonuniform superhydrophilic VACNT (a better description about this phenomena is follow discussed in equations 1-7). In this stage, bath temperature and superficial area were both essential to determine the

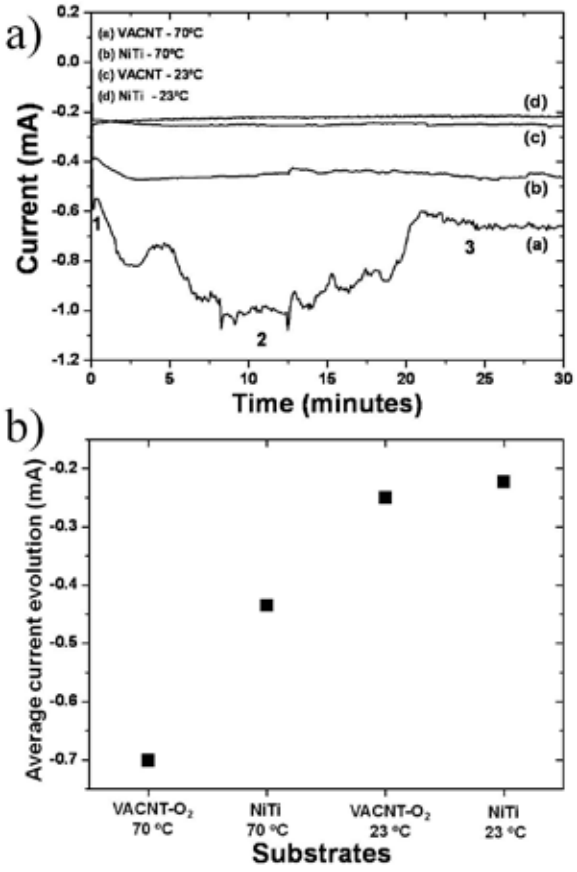

Figure 1: (a) Current-time profile during the deposition of HA films on superhydrophilic VACNT films and NiTi alloys in 0.042 $molL^{-1}$ $Ca(NO_3)_2.4H_2O$ + 0.025 $molL^{-1}$ $(NH_4)_2HPO_4$ solution. Applied potential of -2.0 V (*vs.* Ag/AgCl), and solution temperature kept at 23 and 70°C. (b) Differences of average current evolution of HA films electrodeposition on superhydrophilic VACNT films and NiTi alloys in solution temperature kept at 23 and 70°C.

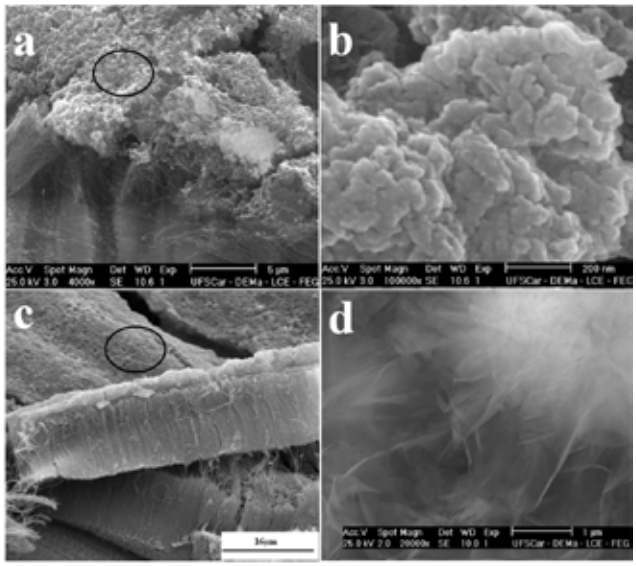

Figure 2: SEM images of direct electrodeposition of HA on superhydrophilic VACNT films at two bath temperatures (a-b) 23 and (c-d) 70ºC. (b) Details of amorphous phosphate formed at 23ºC and (d) HA crystals formed on superhydrophilic VACNT at 70ºC.

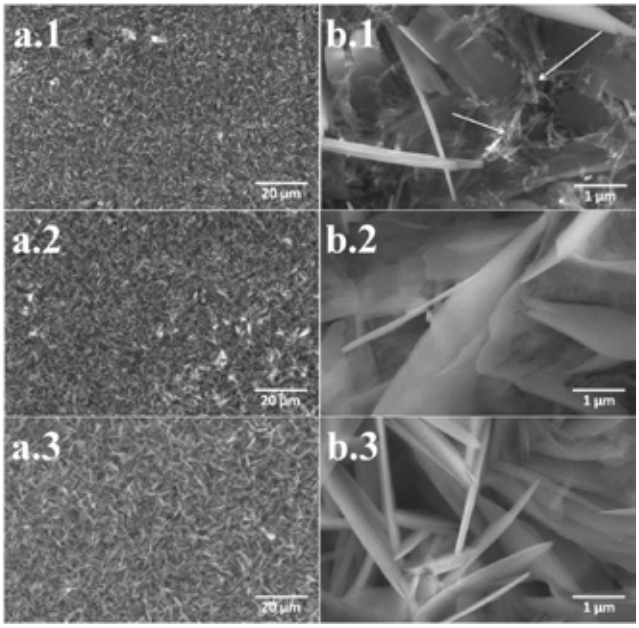

Figure 3: SEM images show the direct electrodeposition of HA on superhydrophilic VACNT films in different times at 70ºC. (a.1 and b.1) 20, (a.2 and b.2) 30, and (a.3 and b.3) 120 minutes.

difference in current values of superhydrophilic VACNT substrates. The superhydrophilic VACNT substrates had current values three times higher than (-1.0 mA) NiTi surfaces. After around 10 min, the current decreased to a limit value, which indicates that the OH^- ion generation process was limited by diffusion (region 3) due to a monolayer of HA crystal formation on superhydrophilic VACNT films. In an electrochemical process, involving the formation of HA, the hydroxyl ion generation on the surface of interest is one of the fundamental parameters to control HA characteristics. Hydroxyl ions induce the acid-base reactions to form PO_4^{-3} and HPO_4^{-2}, which are responsible for leading calcium phosphate precipitation on superhydrophilic VACNT films. All the reactants needed for Ca-P formation, including Ca^{+2}, PO_4^{-3}, HPO_4^{-2}, and OH^- ions, are available [24,25].

The different current among temperatures and substrates are evident. This difference could, in principle, be related to the high concentration of ions in the solution at 70°C, which increases the driving force for diffusion-related phenomena [26]. It is well-known that changes in the surface state of substrate, in the overpotential, may affect the shape of current transient significantly [27]. Current transients may represent different electrochemical processes that take place. The SEM images show the different shape of current transients, which represent a difference in the nature of HA crystal formed.

These electrodeposition process of HA films with increasing deposition temperature can be explained by three factors. First, the solubility HA decreases with increasing temperature [27]. Thus, the particle nucleation rate will also increase, making Ca- P formation more likely to occur close to superhydrophilic VACNT films. Film deposition over bulk precipitation requires the hydroxide to diffuse away from the surface. Second, a higher deposition temperature encourages the deposition of more crystalline film. Ban and Maruno previously reported that the deposition temperature up to 37°C is required to obtain crystalline Ca-P films [28]. Third, as the temperature increased, fewer hydrogen bubbles were found to attach to VACNT surface, so Ca-P film was less damaged. A possible explanation for attachment of fewer hydrogen bubbles is that they are held on the substrate surface by surface tension, and this force decreases with increasing temperature.

HA crystal electrodeposition on superhydrophilic VACNT was performed at different times. Figure 3 shows HA crystal morphologies and density on superhydrophilic VACNT films after 20 (a.1 and b.1), 30 (a.2 and b.2), and 120 (a.3 and b.3) minutes of electrodeposition at 70ºC. Nevertheless, only HA crystal density differences were observed. Details of this lower density can be seen after 20 minutes (Figure 3b.1) due to CNT exposition (white arrows). All images show that HA crystal exhibits polygonal and plate-like shapes. The high level of porosity observed in all the structures may be related to the formation of bubbles during the electrodeposition process. The coating surface exhibits different crystal characteristics and orientation. Regular flake-like structures diverge from the center toward the periphery. The lamellar and plate-like crystal shapes do not show any regular orientation. Details of crystal (length of 1-3 µm and thickness of 1-3 nm) shape and orientation appear in all the images regardless of electrodeposition time. The SEM recordings showed that HA crystals are formed on superhydrophilic VACNT films, which suggests that both the presence of superhydrophilic and nanostructure tip characteristics of VACNT affect nucleation and crystal growth of HA crystals. Morphological changes can be attributed to interactions between oxygen-containing groups and nano-topography of superhydrophilic VACNT films.

The elemental composition of coating was investigated by EDS analysis of HA crystals grown on superhydrophilic VACNT (Figure 4) at 23 and 70°C. The intense peak of Ca, P, and O only shows the presence of strong HA crystal coating over the substrate. The Ca/P ratio determined from the analysis at 70°C was 1.64. The Ca/P value obtained at 23ºC was 0.93 (amorphous phase). The value presented by HA crystals obtained from bath temperature at 70ºC was near stoichiometric HA (1.67) presented in bone tissue [29]. EDS analysis also confirmed the bioactivity and biomineralization process of VACNT/HA composites.

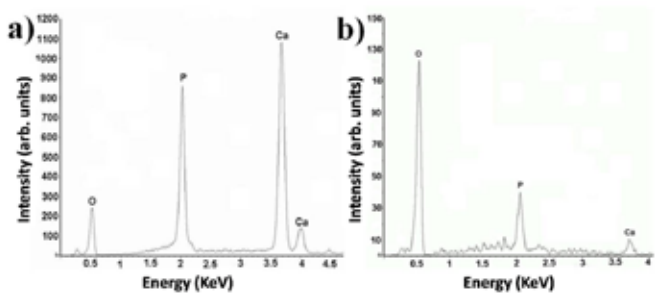

Figure 4: Energy-dispersive x-ray spectrum of HA electrodeposited on superhydrophilic VACNT films at (a) 70 and (b) 23°C.

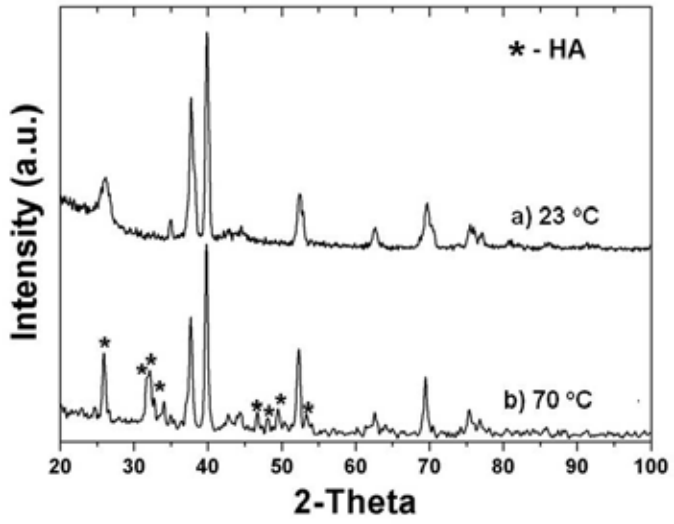

Figure 5: X-ray diffractograms of HA crystals directly formed on superhydrophilic VACNT after electrodeposition two bath temperatures (a) 23 and (b) 70°C.

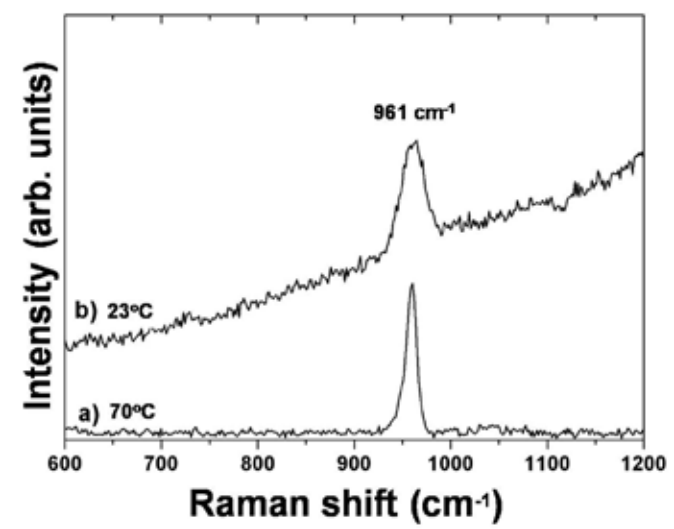

Figure 6: Raman spectra of HA crystals obtained on the superhydrophilic VACNT in solution temperature kept at (a) 23 and (b) 70°C.

A comparison between x-ray diffraction patterns of HA/VACNT obtained at 23°C (a) and HA/VACNT composites at 73°C (b) are shown in Figure 5. Diffraction peaks of VACNT films were observed in both diffractograms. No crystalline phase was observed by HA/VACNT composites obtained at 23°C (Figure 5b). Apatite formation is deduced from the presence of several characteristic x-ray reflection peaks in diffraction pattern shown in Figure 5b. The main diffraction peaks of HA appear at 2Θ values of 25.9° for reflection (002), at 31.9° (triplet) for reflections (211), (112) and (300), and at 34.0° for reflection (200) [30]. This observation backs up the finding on the presence of HA crystals strongly oriented along the c-axis [30].

Figure 6 shows the Raman spectra of HA obtained on the superhydrophilic VACNT films in solution temperature kept at 23 and 70°C. The sharp band at 961cm^{-1} is characteristic of crystalline HA [31]. The amorphous calcium and phosphorus grown on superhydrophilic VACNT in solution (23°C) do not show crystalline HA phase; it only shows the large peaks and a higher luminescent background characteristic to amorphous phase of CO^{3-} and PO^{4}. The film was calculated using deconvolution of lorentizian curves. The higher crystallinity is evident due to the lower band film of 12.5cm^{-1} presented by hidroxyapatite crystals grown on superhydrophilic VACTN in solution (70°C). These findings were associated with the FEG-SEM images to prove the higher crystallinity of HA grown on superhydrophilic VACNT films in solution (70°C).

Liao et al. [32] suggested that dispersed VACNT provides abundant sites for the nucleation of HA in phosphate solution. They showed that bamboo-like structure can be associated to nucleation sites for HA formation. In comparison to the by Liao et al., we have shown that only tip structures of superhydrophilic VACNT films were associated with nucleation of HA crystals. The results are absolutely reproducible and the films are homogeneous throughout the whole deposition surface.

The mechanism of formation HA crystals on superhydrophilic VACNT films are proposed and discussed. The addiction of (NH_4) H2PO4 and Ca (NO_3) produce NH_4NO_3 by equation (1), a very soluble compound [33] whose ions do not participate in the HA reaction deposition.

$$2(NH_4)H_2PO_4 + Ca(NO_3)_2 \rightarrow 2NH_4NO_3 + Ca^{2+} + 2H_2PO_4^- \quad (1)$$

$$2H_2O + 2e^- \rightarrow H_2 + 2OH^- \quad (2)$$

The production of HA needs OH^- ions that come from water molecules hydrolyses. The main equation to produce HA becomes as shown in equation (3).

$$10Ca^{2+} + 6H_2PO_4^- + 14OH^- \rightarrow Ca_{10}(PO_4)_6(OH)_2 + 12H_2O \quad (3)$$

The production of OH^- ions according to equation (3) induces to acid-base reactions leading to production of PO_4^{-3} and HPO_4^{-2} according to equation (4) and (5) respectively. Probably, water reduction (equation (2)) occurs in the crystallographic site, where PO_4^{3-} and OH^- will be discharged by equations (6) and (7), that are the results of equation (2) and (4) addition and equation (2) and (6) addition respectively. Equations (6) and (7) explain the large quantity of H_2 produced in the experiment.

$$H_2PO_4^- + OH^- \rightarrow HPO_4^{2-} + H_2O \quad (4)$$

$$HPO_4^{2-} + OH^- \rightarrow PO_4^{3-} + H_2O \quad (5)$$

$$H_2PO_4^- + H_2O + 2e- \rightarrow HPO_4^{2-} + H_2 + OH^- \quad (6)$$

$$HPO_4^{2-} + H_2O + 2e- \rightarrow PO_4^{3-} + H_2 + OH^- \quad (7)$$

It means that Ca^{+2} cations are transported to the interface from the OH^{-} anions when diffused through the electrolyte [16]. This condition is satisfactory to obtain more homogeneous crystals with activation and it confirms that the drop of electric field on deposited areas promotes deposition on defect regions [16]. In this case, the superhydrophilic VACNT tips can be considered as active sites of defects to crystals grown.

The process for the deposition of HA is originated by an increase of pH in the interface electrolyte/substrate due to ionic charge transfer producing a direct deposition onto substrate. Previous precipitation of calcium phosphate and adsorption of the particles to the substrates induced by electrostatic forces (indirect deposition) may occur. Nevertheless, the preference of a direct growth mechanism can be inferred from several observations (P^{H}, ions concentration, temperature and environment). Three hypothesis about HA electrodeposition process were proposed by other authors [33-36]. The first one is that no charge evolution has been reported for HA particles in basic media [16], which exclude electrostatic forces as responsible for a hypothetical indirect deposition. The second point is associated to adherence of the coatings obtained at low voltages and high temperature, which is related to the diffusion of Ca and specially P through Ti substrate. HA coatings obtained by indirect deposition at higher voltages with sequential sintering temperatures produces also HA films with good adherence. The third point states that the low voltages applied in our experiment lead to current densities comparable to those used by other authors in acidic electrolytes. However, longer times for indirect deposition have been reported [36].

The great novelty of this paper is the direct growth of crystalline HA crystals on superhydrophilic VACNT after the bath control. Generally, the rate of HA crystallization increased with both the current density and the temperature. We have shown that the higher current density observed by superhydrophilic VACNT was sufficient to grown HA crystals without any thermal or surface treatment. The key factor to obtain such crystalline HA crystals was control of superhydrophilic behavior of VACNT films. The same experiments were performed on as grown VACNT films with typical superhydrophobic character and no HA crystals were grown (data not shown). The large surface area of superhydrophilic VACNT enables the interaction of electrolytes and polar functional groups, thereby controlling the crystal growth. The superhydrophilicity itself is very important due to solution wetting of VACNT surface. However, other key characteristic may decisively contribute to HA crystals growth, such as nanostructured tips, -COOH terminal groups, and bamboo-like structures. The superhydrophilicVACNT films obtained from oxygen plasma treatment is modified by the inclusion of polar oxygen surface terminations that may contribute to the hydroxyl ion generation, which is essential in HA electrodeposition process.

Conclusion

The presented results showed that superhydrophilic VACNT films are efficient for growth of HA crystals using an electrodeposition process, and the control of bath is essential to obtain HA with a high degree of crystallinity. Superhydrophilic VACNT films were able to nucleate HA crystals for electrodeposition within twenty minutes resulting in the formation of HA/VACNT nanocomposites.

Acknowledgements

We gratefully acknowledge funding by Fundacao de Amparo a Pesquisa do Estado de Sao Paulo (FAPESP) under the grants 2008/11642-5 and 07/00013-4. The authors are very grateful to Ph.D E.F. Antunes by her assistance in initial parameter development for VACNT grown.

References

1. Qi HJ, Teo KBK, Lau KKS, Boyce MC, Milne WI, et al. (2003) Determination of mechanical properties of carbon nanotubes and vertically aligned carbon nanotube forests using nanoindentation. J Mech Phys Solids 51: 2213-2237.
2. Sawase T, Jimbo R, Baba K, Shibata Y, Ikeda T, et al. (2008) Photo-induced hydrophilicity enhances initial cell behavior and early bone apposition. Clin Oral Implan Res 19: 491-496.
3. Estroff LA, Hamilton AD (2001) Water Gelation by Small Organic Molecules. Chem Mater 13: 3227-3235.
4. Chen Y, Gan C, Zhang T, Yu G (2005) Laser-surface-alloyed carbon nanotubes reinforced hydroxyapatite composite coatings. Appl Phys Lett 86: 251905-251907.
5. Tsui YC, Doyle C, Clyne TW (1998) Plasma sprayed hydroxyapatite coatings on titanium substrates Part 1: Mechanical properties and residual stress levels. Biomaterials 19: 2015-2029.
6. Hukovic MM, Tkalcec E, Kwokal A, Piljac (2003) An in vitro study of Ti and Ti-alloys coated with sol–gel derived hydroxyapatite coatings. J Surf Coat Technol 165: 40-50.
7. Goller G, Demirkiran H, Oktar FN, Demirkesen E (2003) Processing and characterization of bioglass reinforced hydroxyapatite composites. Ceram Int 29: 721-724.
8. Roader RK, Sproul MM, Turner CH (2003) Hydroxyapatite whiskers provide improved mechanical properties in reinforced polymer composites. J Biomed Mater Res A 67: 801-812.
9. Bonfield W, Grynpas MD, Tully AE, Bowman J, Abram J (1981) Hydroxyapatite reinforced polyethylene - A mechanically compatible implant material for bone replacement. Biomaterials 2: 185-186.
10. Berman A, Ahn DJ, Lio A, Salmeron M, Reichert A, et al. (1995) Total Alignment of Calcite at Acidic Polydiacetylene Films: Cooperativity at the Organic-Inorganic Interface. Science 269: 515-518.
11. Shchukin DG, Sukhorukov GB, Möhwald H (2003) Biomimetic Fabrication of Nanoengineered Hydroxyapatite/Polyelectrolyte Composite Shell. Chem Mater 15: 3947-3950.
12. Aryal S, Bhattaraia SR, Remant Bahadur KC, Khil MS, Duck-Rae L, et al. (2006) Carbon nanotubes assisted biomimetic synthesis of hydroxyapatite from simulated body fluid. Mat Sci and Eng A 426: 202-207.
13. Bai Y, Neupane MP, Park IS, Lee MH, Bae TS, et al. (2010) Electrophoretic deposition of carbon nanotubes–hydroxyapatite nanocomposites on titanium substrate. Mater Sci and Eng C 30: 1043-1049.
14. Hahn B-D, Lee J-M, Park D-S, Choi J-J, Ryua J, et al. (2009) Mechanical and in vitro biological performances of hydroxyapatite–carbon nanotube composite coatings deposited on Ti by aerosol deposition. Acta Biomaterialia 5: 3205-3214.
15. Najafi H, Nemati ZA, Sadeguian Z (2009) Inclusion of carbon nanotubes in a hydroxyapatite sol–gel matrix. Cer Inter 35: 2987-2991.
16. Manso M, Jiménez C, Morant C, Herrero P, Martínez-Duart JM (2000) Electrodeposition of hydroxyapatite coatings in basic conditions. Biomaterials 21: 1755-1761.
17. Niu L, Kua H, Chua DHC (2010) Bonelike Apatite Formation Utilizing Carbon Nanotubes as Template. Langmuir 26: 4069-4073.
18. Therese GHA, Kamath PV, Subbann GN (1998) Novel electrosynthetic route to calcium phosphate coatings. J Mater Chem 8: 405-408.
19. Lobo AO, Corat MAF, Ramos SC, Matsushima JT, Granato AEC, et al. (2010) Fast Preparation of Hydroxyapatite/Superhydrophilic Vertically Aligned Multiwalled Carbon Nanotube Composites for Bioactive Application. Langmuir 26: 18308-18314.
20. Antunes EF, Lobo AO, Corat EJ, Trava-Airoldi VJ, Martin AA, et al. (2006) Comparative study of first- and second-order Raman spectra of MWCNT at visible and infrared laser excitation. Carbon 44: 2202-221
21. Antunes EF, Lobo AO, Corat EJ, Trava-Airoldi VJ (2007) Influence of diameter in the Raman spectra of aligned multi-walled carbon nanotubes. Carbon 45: 913-921.

22. Lobo AO, Corat MAF, Antunes EF, Palma MBS, Pacheco-Soares C, et al. (2010) An evaluation of cell proliferation and adhesion on vertically-aligned multi-walled carbon nanotube films. Carbon 48: 245-254.

23. Ramos SC, Vasconcelos G, Antunes EF, Lobo AO, Trava-Airoldi VJ, et al. (2010) Wettability control on vertically-aligned multi-walled carbon nanotube surfaces with oxygen pulsed DC plasma and CO2 laser treatments. Diam Relat Mater 19: 52-755.

24. Barrere F, Snel MME, Blitterswijka A, de Klaas G, Layrolle P (2004) Nanoscale study of the nucleation and growth of calcium phosphate coating on titanium implants. Biomaterials 25: 2901-2910.

25. Ma J, Wang C, Peng KW (2003) Electrophoretic deposition of porous hydroxyapatite scaffold. Biomaterials 24: 3505-3510.

26. Elliot JC (1994) Structure and chemistry of the apatites and other calcium orthophosphates. Elsevier, Amsterdam Chapter 3.

27. Lu X, Zhao Z, Leng Y (2005) Calcium phosphate crystal growth under controlled atmosphere in electrochemical deposition. J Crystal Growth 284: 506-516.

28. Ban S and Hasegawa J (2002) Morphological regulation and crystal growth of hydrothermal electrochemically deposited apatite. Biomaterials 23: 2965–2972.

29. Mahamid J, Sharir A, Addadi L, Weiner S (2008) Amorphous calcium phosphate is a major component of the forming fin bones of zebrafish: Indications for an amorphous precursor phase. PNAS 105: 12748-12753.

30. Klug HP, Alexander LE (1954) X-ray Diffraction Procedures. John Wiley, New York.

31. Kale S, Biermann S, Edwards C, Tarnowski C, Morris M, et al. (2000) Three dimensional cellular development is essential for ex vivo formation of human bone. Nature Biotechnol 18: 954-958.

32. Liao S, Xu G, Wang W, Watari F, Cui F, et al. (2007) Self- assembly of nano-hydroxyapatite on multiwalled carbon nanotubes. Acta Biomater 3: 669-675.

33. Patnaik P. Handbook of inorganic chemicals. McGraw-Hill, 2003, ISBN: 070494398.

34. Pezzatini S, Solito R, Morbidelli L, Lamponi S, Boanini E, et al. (2006) The effect of hydroxyapatite nanocrystals on microvascular endothelial cell viability and functions. J Biomed Mater Res A 76: 656-663.

35. Damodaran, Moudgil BM (1993) Electrophoretic deposition of calcium phosphates from non-aqueous media. Colloid Surf A: Physicochem Eng Aspects 80: 191-195.

36. Redepenning J, Schlessinger T, Burnhum S, Lipiello L, Miyano J (1996) Characterization of electrolytically prepared brushite and hydroxyapatite coating on orthopaedic alloys. J Biomed Mater Res 30: 287–294.